J. Fluid Mech. (1975), *vol.* 68, *part* 3, *pp.* 477–495
Printed in Great Britain

The instability of capillary jets

By ARTHUR M. STERLING† AND C. A. SLEICHER
Department of Chemical Engineering, University of Washington, Seattle

(Received 28 March 1974)

At high jet velocity the aerodynamic interaction between a capillary jet and the surrounding medium leads to an enhanced growth rate of axisymmetric disturbances. The available theories which account for this effect fail to agree with experimental observations. The difference is attributed, in part, to the relaxation of the velocity profile in jets formed by fully developed laminar pipe flow. The profile relaxation has a destabilizing effect just as does the aerodynamic interaction. In the absence of velocity-profile relaxation it is shown that the available theories overestimate the aerodynamic effect. A consideration of the viscosity of the ambient fluid yields a semi-empirical modification to the theory which shows good agreement with experimental values.

1. Introduction

It is a well-known and common observation that when a jet of liquid issues from an orifice or nozzle into air it always breaks up into a train of drops. The breakup process is primarily a result of capillary instability, and its mathematical description was given by Rayleigh (1878). A more complete description of the capillary instability of Newtonian liquid jets at low velocities was given by Weber (1931), who has also shown that the behaviour of jets at higher velocities is affected by the aerodynamic forces at the jet–air interface. These forces enhance the growth rate of a disturbance and lead to a nonlinear relation between the continuous length of the jet and its velocity. Weber's theory predicts that the length will reach a maximum at some critical jet velocity. The predicted values of the maximum jet length and the critical velocity fail to agree, however, with available experimental data. This has led previous investigators either to modify empirically (with little success) or to discount entirely Weber's theory of aerodynamic interaction.

Weber's theory has not, in fact, been fairly tested. In the main, experiments used to test this theory have been carried out with nozzles of sufficient length to ensure fully developed laminar pipe flow. This in turn introduces the complication of velocity-profile relaxation, which is not taken into account by the theory and which can have a marked effect on the instability.

The objectives of this work are twofold.

(i) To test Weber's theory through an investigation of jets which are influenced by aerodynamic forces but are free from the effects of velocity-profile

† Present address: Afdeling Urologie, Academisch Ziekenhuis Leiden, Leiden, The Netherlands.

relaxation. The results will show that Weber's theory overestimates the aerodynamic effects.

(ii) To consider the effect of ambient fluid viscosity on the normal stresses at the jet surface. The result, together with the results of the experiments, will be used to modify Weber's theory of aerodynamic interaction.

2. Theory

Consider a column of fluid of density ρ, viscosity μ and surface tension σ streaming with uniform velocity U through a stationary, inviscid, incompressible medium of density $\hat{\rho}$. The column is assumed to be infinite in the axial direction and of radius a. We take a cylindrical polar co-ordinate system (r, θ, z) which moves with the column of fluid; the z axis coincides with the axis of the column and its positive direction is opposite to that of the uniform flow.

We impose upon this initially steady motion an arbitrary, small, axisymmetric disturbance one Fourier component of which has at the surface the form

$$\eta = \mathscr{R}(\eta_0 e^{\beta t + ikz}). \tag{1}$$

In (1), η represents the displacement of the surface in the radial direction from its undisturbed position $r = a$, t is time, η_0 is the initial amplitude, $k = 2\pi/\lambda$ is the wavenumber, λ is the wavelength and β is the complex frequency. The real part of β is the growth rate of the disturbance. There is no loss of generality in restricting the disturbance to be axisymmetric for only axisymmetric disturbances are unstable.

Associated with the disturbance will be a small axisymmetric fluctuating pressure p and velocity $\mathbf{u}$ (with axial and radial components u and v). These fluctuations are described by the equations of motion and continuity, which can be linearized by neglecting all terms of second order in the fluctuating quantities. In our co-ordinate system the linearized equations are

$$\frac{\partial \mathbf{u}}{\partial t} = -\frac{1}{\rho}\nabla p + \frac{\mu}{\rho}\nabla^2 \mathbf{u}, \tag{2}$$

$$\nabla . \mathbf{u} = 0. \tag{3}$$

The boundary conditions to be applied at the surface, which can be taken as $r \simeq a$ to first order in η, require that there be no net flux of mass across the surface, that the shear stress be zero and that the normal stress be continuous. These boundary conditions are expressed as

$$v = \partial\eta/\partial t \quad \text{at} \quad r \simeq a, \tag{4}$$

$$\partial u/\partial r + \partial v/\partial z = 0 \quad \text{at} \quad r \simeq a, \tag{5}$$

$$-(P+p) + 2\mu\frac{\partial v}{\partial z} = -\hat{p} - \sigma\left(\frac{1}{R_1} + \frac{1}{R_2}\right) \quad \text{at} \quad r \simeq a, \tag{6}$$

where P is the undisturbed pressure in the jet and is equal to σ/a, $\hat{p}$ is the fluctuating pressure in the surrounding medium and R_1 and R_2 are the principal radii of curvature of the surface. It is easily shown that to first order in η

$$\frac{1}{R_1} + \frac{1}{R_2} \simeq \frac{1}{a} - \frac{1}{a^2}(1 - k^2a^2)\eta.$$

We note that the inertial effects of the surrounding medium enter our analysis only through the fluctuating pressure $\hat{p}$ in boundary condition (6). This pressure is found from the equations of motion and continuity for the surrounding medium, which are

$$\frac{\partial \hat{\mathbf{u}}}{\partial t} + U\frac{\partial \hat{\mathbf{u}}}{\partial z} = -\frac{1}{\hat{\rho}}\nabla\hat{p}, \tag{7}$$

$$\nabla . \hat{\mathbf{u}} = 0, \tag{8}$$

with the boundary condition

$$\hat{v} = \partial\eta/\partial t + U\,\partial\eta/\partial z \quad \text{at} \quad r \simeq a. \tag{9}$$

We continue with the notation that quantities which refer to the surrounding medium are indicated with a caret with the exception of U, whose meaning is clear. As we have assumed that the surrounding medium is inviscid, we can express the velocity in terms of a velocity potential, i.e. we can take $\hat{\mathbf{u}} = \nabla\hat{\phi}$, which reduces (7) and (8) to

$$\partial\hat{\phi}/\partial t + U\,\partial\hat{\phi}/\partial z = -\hat{p}/\hat{\rho} \tag{10}$$

and

$$\nabla^2\hat{\phi} = 0. \tag{11}$$

Within the jet the velocity can be separated into an irrotational and viscous part, i.e.

$$\mathbf{u} = \nabla\phi + \nabla\times\mathbf{B},$$

where ϕ is the velocity potential, $\mathbf{B} = (0, -\psi/r, 0)$ and ψ is the stream function, defined by

$$u = -\frac{1}{r}\frac{\partial\psi}{\partial r}, \quad v = \frac{1}{r}\frac{\partial\psi}{\partial z}.$$

This reduces (2) and (3) to

$$\partial\phi/\partial t = -p/\rho, \tag{12}$$

$$\frac{\partial^2\psi}{\partial r^2} - \frac{1}{r}\frac{\partial\psi}{\partial r} + \frac{\partial^2\psi}{\partial z^2} - \frac{\mu}{\rho}\frac{\partial\psi}{\partial t} = 0, \tag{13}$$

$$\frac{\partial^2\phi}{\partial r^2} + \frac{1}{r}\frac{\partial\phi}{\partial r} + \frac{\partial^2\phi}{\partial z^2} = 0. \tag{14}$$

In terms of $\hat{\phi}$, ϕ and ψ, the boundary conditions (4)–(6) and (9) become

$$\frac{\partial\hat{\phi}}{\partial r} = \frac{\partial\eta}{\partial t} + U\frac{\partial\eta}{\partial z} \quad \text{at} \quad r \simeq a, \tag{15}$$

$$\frac{\partial\phi}{\partial r} + \frac{1}{r}\frac{\partial\psi}{\partial z} = \frac{\partial\eta}{\partial t} \quad \text{at} \quad r \simeq a, \tag{16}$$

$$\frac{1}{r}\frac{\partial^2\psi}{\partial z^2} - \frac{\partial}{\partial r}\left(\frac{1}{r}\frac{\partial\psi}{\partial r}\right) + 2\frac{\partial^2\phi}{\partial r\,\partial z} = 0 \quad \text{at} \quad r \simeq a, \tag{17}$$

$$-p + 2\mu\frac{\partial^2\phi}{\partial r^2} = -\hat{p} + \frac{\sigma}{a}(1-k^2a^2)\eta \quad \text{at} \quad r \simeq a. \tag{18}$$

We now assume $\hat{\phi}$, ϕ and ψ to be of the form

$$g(r, z, t) = G(r)\,e^{\beta t + ikz}$$

and seek solutions of (11), (13) and (14) which are free from singularities at the axis and at infinity. These solutions are

$$\hat{\phi} = AK_0(kr)\,e^{\beta t+ikz}, \quad \phi = BI_0(kr)\,e^{\beta t+ikz},$$
$$\psi = CrI_1(lr)\,e^{\beta t+ikz},$$

where $I_n(kr)$ and $K_n(kr)$ are the nth-order modified Bessel functions of the first and second kind and $l^2 = k^2+\beta\rho/\mu$. The constants A, B and C are eliminated through the boundary conditions (15)–(17) and the pressures p and $\hat{p}$ are found from the equations of motion (10) and (12). Substitution into the normal-stress boundary condition (18) yields, after considerable algebraic manipulation,

$$\beta^2\left\{\frac{\xi I_0(\xi)}{2I_1(\xi)}+\frac{\hat{\rho}\xi K_0(\xi)}{2\rho K_1(\xi)}\right\}$$
$$+\beta\left\{2i\frac{U\hat{\rho}\xi^2K_0(\xi)}{2\rho aK_1(\xi)}+\frac{\mu\xi^2}{\rho a^2}\left[2\xi\frac{I_0(\xi)}{I_1(\xi)}-1+\frac{2\xi^2}{\xi_1^2-\xi^2}\left(\xi\frac{I_0(\xi)}{I_1(\xi)}-\xi_1\frac{I_0(\xi_1)}{I_1(\xi_1)}\right)\right]\right\}$$
$$=\frac{\sigma}{2\rho a^3}(1-\xi^2)\,\xi^2+\frac{U^2\hat{\rho}\xi^3K_0(\xi)}{2a^2\rho K_1(\xi)}, \tag{19}$$

or
$$\beta^2\{F_1\}+\beta\{iF_2+F_3\} = F_4+F_5, \tag{20}$$

where
$$\xi = ka, \quad \xi_1^2 = \xi^2+\beta a^2\rho/\mu.$$

Equation (19) includes the results of all previous investigators as special cases. Specifically, with $\hat{\rho}$, μ and U equal to zero, (19) reduces to

$$\beta^2 = \frac{\sigma}{\rho a^3}(1-\xi^2)\frac{I_1(\xi)}{I_0(\xi)},$$

a result due originally to Rayleigh. If we neglect only the viscosity of the jet, i.e. set $F_3 = 0$, there remains a slightly different form of the result obtained by Alterman (1961), which is the solution for a cylindrical vortex sheet with surface tension. Since β will now be complex, the disturbance will propagate along the jet with a velocity $c = \beta_i/k$, where β_i is the imaginary part of β. Recall that, with c positive, the direction of propagation will be opposite to the direction of motion of the jet.

Finally, if we neglect only the imaginary term F_2, we obtain the result due to Weber. Weber further simplified the equation with the approximations

$$\frac{\hat{\rho}}{\rho}\frac{\xi K_0(\xi)}{2K_1(\xi)} \ll \frac{\xi I_0(\xi)}{2I_1(\xi)},$$

and for $\xi < 1$,
$$\xi I_0(\xi)/2I_1(\xi) = 1{\cdot}0.$$

The simplified result is

$$\beta^2+\frac{3\mu\xi^2}{\rho a^2}\beta = \frac{\sigma}{2\rho a^3}(1-\xi^2)\,\xi^2+\frac{U\hat{\rho}\xi^3K_0(\xi)}{2a^2\rho K_1(\xi)}. \tag{21}$$

In treating the influence of the air on the growth of the disturbance, Weber considered the flow of air over a corrugated cylinder. For a fixed surface the term F_2 does not arise and was therefore not included by Weber. If the corrugations are allowed to grow, however, this term does arise. Though it is clear that

this term contributes an imaginary component to β, i.e. a disturbance velocity relative to the jet velocity, it is difficult to assess, by inspection, its effect on the results for the maximum value of β and the wavenumber at which β is a maximum. Calculations were carried out by the authors on the full equation (19) for a variety of fluids and jet diameters and compared with the results when F_2 was omitted. These calculations show that in all cases the term in question could be ignored as it contributes little to the magnitude of β (less than 0·1 %), and the calculated wave velocity is less than 0·2 % of the relative velocity between the jet and the ambient fluid.

The criterion for the truncation of the Bessel functions used to reduce (19) to (21) is that the argument be less than unity. This criterion is satisfied for ξ but not necessarily for ξ_1. A comparison of solutions of (19) with those of (21) for low velocity water jets, however, shows a small difference in the maximum value of β ($\sim 3\,\%$) and a negligible difference in the wavenumber at which the maximum occurs. It should be noted that when the aerodynamic term F_5 becomes appreciable β is larger. Thus ξ_1 is also larger, and the difference between the solutions of (19) and (21) may become appreciable. Because of this effect, the curves for Weber's equation shown on figures 4–8 below were derived from the full equation (19).

Experimental tests of the characteristic equation

The properties of the jet which are of most interest are either the drop size or spacing (a measure of the wavenumber of the most unstable disturbance) and the continuous length (a measure of the growth rate of the disturbance).

If the amplitude of all the Fourier components of the arbitrary initial disturbance are of the same order of magnitude, it is expected that the component with the largest growth rate will eventually dominate the breakup. We denote the dimensionless wavenumber of this component as ξ^* and the growth rate of this component as β^*. If the initial disturbance has amplitude η_0 and grows to a magnitude a in time t^*, then

$$a = \eta_0 e^{\beta^* t^*},$$

or

$$t^* = \beta^{*-1} \ln (a/\eta_0).$$

The jet length will then be

$$L = Ut^* = (U/\beta^*) \ln (a/\eta_0). \tag{22}$$

The most unstable wavenumber ξ^* and the growth rate β^* are obtained from the solution of (19) or (21). Substitution of β^* into (22) yields a theoretical jet length which, together with ξ^*, can be compared with experimentally determined values.

3. Modification of the theory

Previous modifications

Grant & Middleman (1966) performed a series of careful experiments on liquid jets with a wide range of viscosities from nozzles with length-to-diameter ratio $l/d \simeq 100$. They were unable to correlate their data with Weber's result. For jets

with Ohnesorge number $Z = \mu/(\rho d\sigma)^{\frac{1}{2}}$ less than 0·056 the jet length and jet velocity at maximum length were less than those predicted; for jets with Z greater than 0·056 the converse was found. They then modified Weber's result in two steps. First, the aerodynamic term F_5 in (20) was modified by replacing the Bessel functions with an arbitrary function of the Ohnesorge number. That is, they put

$$F_5 = (\hat{\rho}U^2/\rho a^2)\,\xi^3 f(Z).$$

By forcing the modified equation to predict velocities at the maximum jet length which were consistent with their data, they found

$$f(Z) = C_1 Z^{-1\cdot 32}.$$

As a second step, the jet length predicted by the modified theory was forced to agree with experiment by treating the magnitude of the initial disturbance in (22) as a function of Z. This resulted in

$$\ln(a/\eta_0) = C_2 - C_3 \ln Z.$$

This empirical modification correlated their experimental results at standard pressures, but it failed for data taken at reduced ambient pressures. The jet lengths predicted by the modified theory for subatmospheric pressures are much greater than those observed experimentally. No data were reported on the wavenumber of the dominant disturbance.

The failure of Grant & Middleman's correlation at reduced pressures has implications for the physical mechanisms involved in the breakup. The term which they modified arises, in the theory, solely from a consideration of the inertia of the ambient fluid. Their modification, however, is made in terms of properties of the jet fluid only and therefore must correct for physical processes which occur within the jet. The modified term retains the ambient density, and as the ambient pressure is reduced, the correlation is lost. One must conclude that the primary mechanism responsible for the maximum in Grant & Middleman's breakup curves is connected with processes occurring within the jet and is independent of ambient conditions. One plausible process is the relaxation of the fully developed laminar velocity profile, the effects of which can be related heuristically to Grant & Middleman's correlation in the following way.

On the basis of measurements of the centre-line stagnation pressure in jets initially in fully developed laminar flow, Rupe (1962) suggests that the jet length required for the velocity profile to relax to a uniform velocity profile (the relaxation length) is comparable with the entry length for laminar flow in a pipe. This agrees quite well with the theoretical results due to Bohr (1909) and Duda & Vrentas (1967). Thus we take

$$l_r/d \propto Re,$$

where l_r is the relaxation length.

We can estimate the parametric dependence of the breakup length using (21) and (22). In the absence of aerodynamic effects these equations give

$$L/d \propto We^{\frac{1}{2}}(1+3Z),$$

from which

$$l_r/L \propto 1/(Z+3Z^2).$$

The effect of the velocity-profile relaxation should become more pronounced as the ratio of relaxation length to breakup length increases. We also expect the relaxation effects to depend on the extent to which the velocity profile differs from a uniform profile. A convenient measure of this difference is the velocity gradient at the wall:

$$[\partial U/\partial r]_{r=a} \propto U/a.$$

One might then expect the velocity-profile relaxation effects to increase in proportion to the product

$$(U/a)^2(Z+3Z^2)^{-1}, \tag{23}$$

whose units are consistent with the other terms of (19). Grant correlated his results with a term of the form

$$\text{constant}\,(U/a)^2 Z^{-1\cdot 32}. \tag{24}$$

The similarity of these forms strongly suggests that Grant & Middleman's correlation accounted for velocity-profile relaxation and that an important parameter in such a correlation is the ratio of relaxation length to breakup length. When the relaxation length is small compared with the breakup length, i.e. Z is large, velocity-profile relaxation effects should be small, and the aerodynamic forces should determine the nonlinear behaviour. Conversely, when Z is small, relaxation effects become paramount, rendering the breakup curve independent of the ambient conditions. Such arguments are consistent with the available experimental data.

Grant & Middleman's correlation for the initial amplitude of the disturbance in terms of the Ohnesorge number corrects for jet length in a way opposite to the modification of the aerodynamic term. That is, as Z increases, the growth rate calculated from the modified equation is less, which increases the jet length according to (22). The correlation for $\ln(a/\eta_0)$, however, indicates a decrease in jet length as Z increases. In this connexion we note the functional behaviour of the forms (23) and (24). Apart from a constant multiplier, which is unimportant here, the form (23) has smaller values at low Z and higher values at large Z. Thus the use of (23) in Grant & Middleman's modification would lead to longer jet lengths at small Z and shorter jet lengths at large Z, a correction which acts in the same way as their correlation for $\ln(a/\eta_0)$. It would be interesting to see whether this new functional dependence on Z could alone account for the relaxation effects.

Proposed modification

Any improvement to the theory with respect to the aerodynamic forces must centre about the effects of the viscosity of the ambient fluid, for the neglect of the viscosity of the ambient fluid is the most significant simplifying assumption of Weber's analysis. The viscous effects enter the analysis through the shear-stress and normal-stress boundary conditions at the jet surface. (In the derivation of (19), the shear stress was set to zero and the normal stress imposed by the ambient fluid was taken as the negative of the ambient static pressure. This is found, through (7) and (9), to be in exact antiphase with the elevation of the surface of

the jet.) In principle, these stresses can be determined for the viscous case from the solution of the cylindrical form of the Orr–Sommerfeld equation, which describes shearing flow over a wavy cylinder. This is a difficult task, but we can gain some insight into the form of these stresses by considering previous results obtained for the planar case.

Benjamin (1959) has treated the case of shearing flow over a two-dimensional wavy surface. For thin boundary layers (of thickness small compared with the wavelength of the disturbance) over a surface on which waves move slowly in the direction of the primary flow, the energy transferred from the mean flow to the disturbance by shear stresses is small compared with the energy transferred by normal stress, and the ratio is independent of the Reynolds number. In the limit as the Reynolds number tends uniformly to infinity, the pressure distribution at the boundary is "that given by the ideal-fluid theory applied to the (Kelvin–Helmholtz) model of a uniform primary flow extending right down to the boundary". For a finite Reynolds number Benjamin finds that the magnitude of the fluctuating pressure component in phase with the wave elevation is less than the magnitude given by the ideal-fluid theory.

As a first approximation, we can apply these results directly to the present case. That is, we neglect the shear stress at the jet surface and reduce the magnitude of the normal stress by a coefficient yet to be determined. Equation (19) remains unchanged except that the function F_5 is replaced by the function CF_5. That is, the modified equation becomes

$$\beta^2\{F_1\}+\beta\{iF_2+F_3\} = F_4+CF_5. \tag{25}$$

The constant C can then be determined by comparing the results of (25) and (22) with experimentally observed values. Those values must be from experiments in which velocity-profile effects were negligible, and for this purpose we have chosen data reported by Fenn & Middleman (1969) for their solution 2 at a pressure of 0·5 atm. For a given value of C, equation (25) was solved by an iterative technique on a computer. The maximum value of the growth rate β^* was found by a 20 step golden-sections search over the possible values of the dimensionless wavenumber. The growth rate was then used with (22) to calculate the jet length. The parameter $\ln(a/\eta_0)$ in (22) was found by using low velocity data, the theory for which is not in question. That is, η_0 depends upon ambient vibrations and noise and the extent to which the apparatus is isolated from such disturbances. The value of $\ln(a/\eta_0)$ found at low velocities was then assumed to apply at the higher velocities. The constant C was adjusted until the calculated and experimental values of the jet length agreed at a velocity of 2510 cm/s. The values agreed when $C = 0{\cdot}175$.

4. Experiment

Apparatus

The experimental apparatus consisted of a pressurized fluid reservoir, a calming section and a fluid receiver, as shown in figure 1. A 15 gallon air receiver vessel was used as the fluid reservoir. The reservoir was pressured by bottled dry

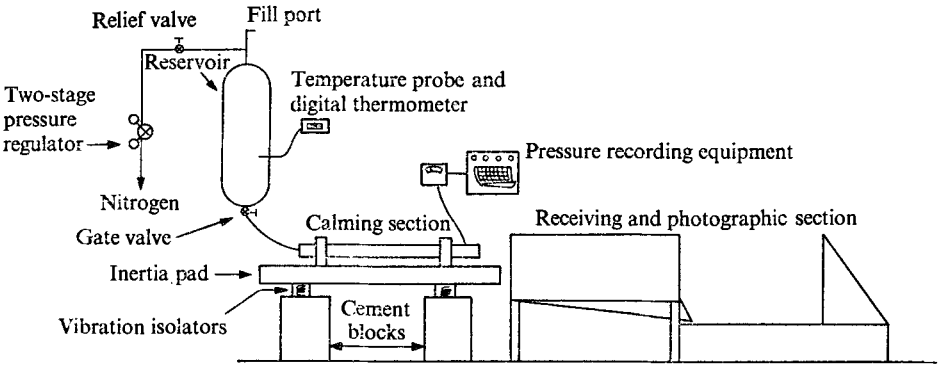

FIGURE 1. Schematic of experimental apparatus.

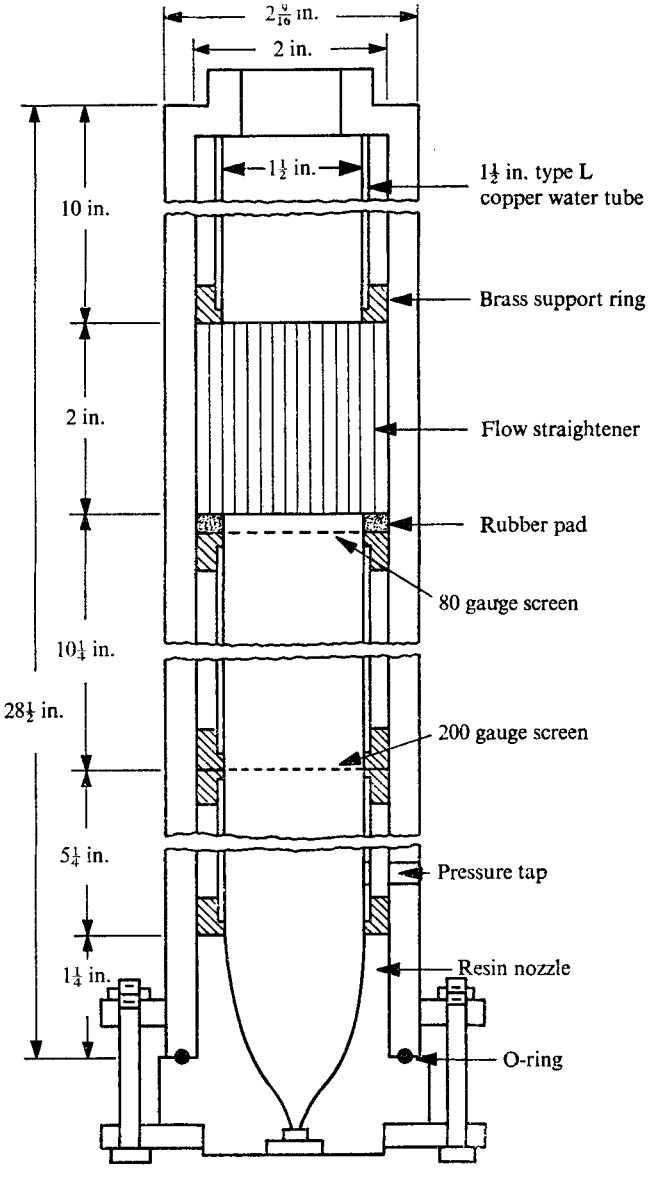

FIGURE 2. Calming section.

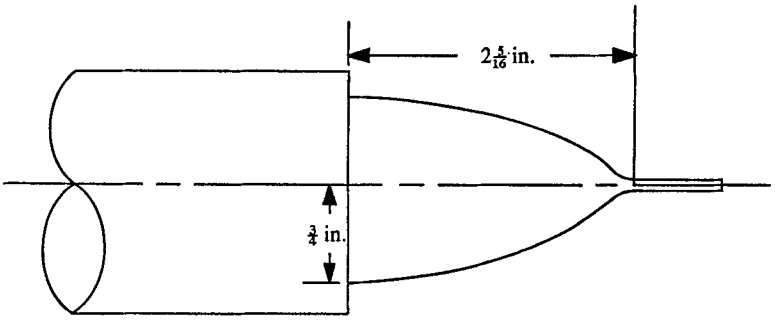

FIGURE 3. Shape of nozzle core.

nitrogen. The fluid temperature was measured by a probe installed in the reservoir and connected to a digital thermometer. Fluid passed from the reservoir to the calming section via a 2 ft flexible hose.

The calming section (figure 2) consisted of a 29 in. length of 2 in. I.D. BWG 3 stainless-steel pressure tubing, which enclosed sections of $1\frac{1}{2}$ in. type L copper water tube and a 2 in. aluminium honeycomb flow straightener. The sections of copper tube were supported by brass rings, two of which were fitted with calming screens. The downstream end of the copper tube butted firmly against the nozzle. A pressure tap was drilled 2 in. from the downstream end of the section, and pressures were measured with a Statham transducer and recorded on a Heathkit chart strip recorder.

The calming section was fixed to a 350 lb cement inertia pad, which rested on four vibration isolators (springs). The vibration isolators were placed on two 3 ft columns of concrete blocks. It should be added that the building itself is relatively vibration free; all motors in the building larger than about 1 h.p. are supported on vibration isolation mounts.

Nozzles were made by casting polyester resin around a polished aluminium core. The core was turned to the shape shown in figure 3 and was designed to give a nearly uniform velocity profile at the nozzle exit. The greatest diameter of the nozzle matched the inside diameter of the copper water tube, and the least diameter matched the desired orifice diameter. Both ends of the core were parallel to the axis of symmetry. The nozzles were initially cast with a short length ($l/d \simeq 1$) of hypodermic tubing embedded in the downstream end. This tubing was carefully removed after the nozzle had cured, leaving a smooth circular orifice. These nozzles are hereafter referred to as short nozzles.

Extensions to the nozzles (hereafter referred to as extended nozzles) were made by inserting a length of hypodermic tubing in place of the short section of tubing which had been removed. The snugness of fit was sufficient to hold the extension in place.

Nozzle diameters were measured by a travelling microscope which was accurate to within 0·001 cm. The dimensions of the nozzles used in this experiment are shown in table 1.

The physical properties of the experimental fluids are given in table 2.

	d (cm)	l/d
Short nozzles	0·238	$\simeq$ 0·25
	0·167	$\simeq$ 0·25
Extended nozzles	0·238	96
	0·160	49

TABLE 1. Nozzle dimensions

	Surface tension (dynes/cm)	Viscosity (cP)	Density (g/cm^3)
Water	72·3	0·93	0·997
Isopropyl alcohol	21·7	2·13	0·784
No. 3 mineral oil	29·4	31	0·868

TABLE 2. Physical properties of the experimental fluids at 23 °C

Data collection

A pressure–velocity correlation was determined for each nozzle–fluid combination. The jet fluid was collected over times long enough to negate timing errors, and the pressure was recorded. The volume flow rate was then converted to the jet velocity at the orifice. The velocity of the jets formed by the extended nozzles was corrected to account for the jet contraction in accordance with the correlation of Gavis & Modan (1967). A similar correction was not applied to the velocity of the jets formed by the short nozzles, for the contraction of these jets, as discussed below, was small.

When the jet was very steady, as it was for lower velocities, the motion could be visually frozen by a strobe light, and the breakup point could be determined accurately. With the room lights on, the jet appeared to thicken and to become opaque at the point where the jet pinched off, indicating the breakup point. It was determined that either of these methods gave sufficiently accurate indications of the breakup point. At intermediate velocities the jet length varied by as much as $\pm$ 2 cm about a mean value. In this case the breakup point was determined in room light as the eye averaged these variations.

Once the breakup point had been determined, the length was measured by a flexible tape, placed so that its curvature approximated the curvature of the jet. At higher velocities, when the variation in length exceeded $\pm$ 2 cm, the average breakup length was determined from photographs taken with a 16 mm Arriflex motion-picture camera on Plus-X film at 24 frames/s. The framing rate was at least an order of magnitude less than the lowest frequency of the variation in jet length. The jets were illuminated from behind by a General Radio Strobotac synchronized to the camera shutter. Fifty to one-hundred frames were exposed at each velocity. The films were read on a Vanguard motion analyser at a net magnification of 0·55. The breakup point was measured with respect to a fiducial point and the jet length recorded.

For the jets formed by the short nozzles, the wavenumbers and contraction ratios (diameter of jet divided by orifice diameter) were measured from still

Velocity (cm/s)	Nozzle diameter (cm)	Reynolds number	Contraction ratio
312	0·167	146	0·953
210	0·280	1841	0·984
1150	0·167	7077	0·988

TABLE 3. Jet-contraction measurements for short nozzles

photographs. These photographs were taken on Tri-X film with a Nikon camera fitted with a 200 mm lens on a bellows extension. A section of tubing of known diameter, placed in the plane of the jet, was included in the photograph. A strobe light, synchronized to the shutter of the camera, illuminated the jets from behind. Films were read on the Vanguard motion analyser at a net magnification of $\times 4$. Wavelengths and jet diameters were measured to within 0·001 cm and recorded.

5. Discussion of results

Performance of short nozzles

The diameters of the jets formed by the short nozzles were measured to test for the presence of contraction owing to either velocity-profile relaxation or separation of the flow. The measurements were made at jet lengths sufficient to ensure complete relaxation of the velocity profile. The results are shown in table 3.

A measure of the effective l/d of the short nozzles can be obtained by comparing the result at the lowest Reynolds number with the results obtained by Gavis & Modan (1967). This comparison indicates that the effective l/d is less than 0·5, and extrapolation of their data indicates a value of the order of 0·25.

The contraction ratio at the highest velocity indicates the absence of a *vena contracta* and is in agreement with the Gavis & Modan result that the contraction ratio for short nozzles approaches unity as the Reynolds number becomes larger.

These results indicate that the short nozzles were adequate to form jets effectively free of separation and velocity-profile relaxation effects.

Breakup curves

The breakup curves for water, isopropanol and mineral-oil jets are presented in figures 4–8. In all cases, the length of the jets formed by the short nozzles is much longer, and the maximum length occurs at a higher velocity than those predicted by Weber's theory, i.e. equation (20).

For the water jets and the isopropanol jet formed by the larger diameter nozzle (figures 4–6), the maximum in the breakup curve can be attributed to a perturbation of the surface by turbulent eddies within the jet. This was indicated by a sudden change in the appearance of the jet at the nozzle from a smooth glassy surface to a semi-opaque ruffled surface. The velocity at which surface ruffling first appeared is indicated in the figures. The Reynolds number at which surface ruffling occurs is not unique but tends to decrease monotonically with increasing

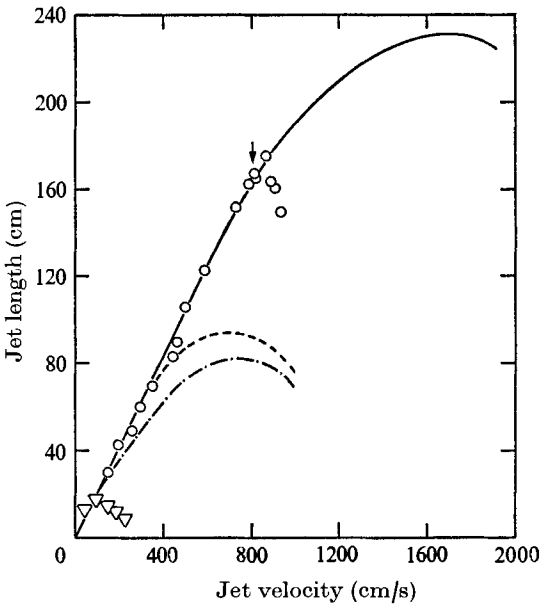

FIGURE 4. Breakup length of water jets as a function of jet velocity and nozzle length-to-diameter ratio. ○, $l/d = 0$; – – – –, Weber's equation; ——, modified equation; ↓ velocity at which surface ruffling first occurs. ▽, $l/d = 96$; — · —, Weber's equation. Nozzle diameter = 0·238 cm.

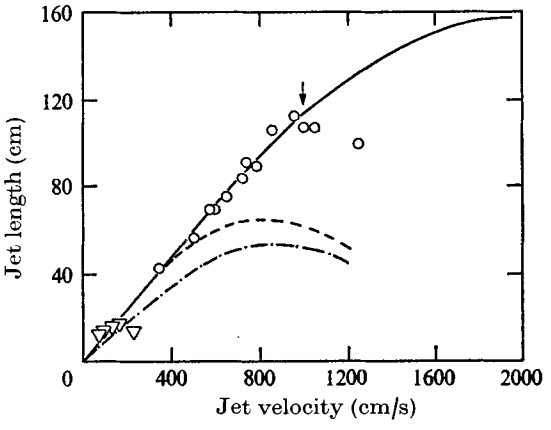

FIGURE 5. Breakup length of water jets as a function of jet velocity and nozzle length-to-diameter ratio. Nozzle diameter = 0·167 cm: ○, $l/d = 0$; – – – –, Weber's equation; ——, modified equation; ↓, velocity at which surface ruffling first occurs. Nozzle diameter = 0·160 cm: ▽, $l/d = 49$; — · —, Weber's equation.

Ohnesorge number Z. In the absence of surface ruffling (figures 7 and 8), the breakup curves exhibit the same general shape as is predicted by Weber's result. This suggests that the form of Weber's result is correct but that the aerodynamic effects are overestimated.

The breakup curves obtained from the extended nozzles are included for comparison in figures 4–8. The maximum in these curves for water and isopropyl

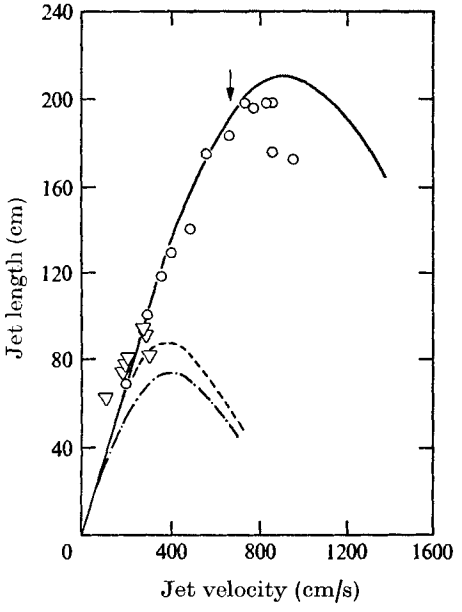

FIGURE 6

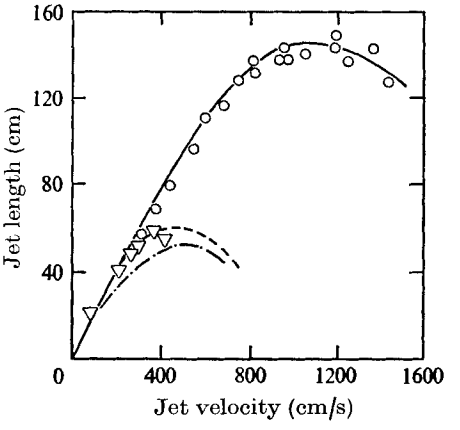

FIGURE 7

FIGURE 6. Breakup length of isopropanol jets as a function of jet velocity and nozzle length-to-diameter ratio. ○, $l/d = 0$; – – –, Weber's equation; ——, modified equation; ↓, velocity at which surface ruffling first occurs. ▽, $l/d = 96$; — — —, Weber's equation. Nozzle diameter = 0·238 cm.

FIGURE 7. Breakup length of isopropanol jets as a function of jet velocity and nozzle length-to-diameter ratio. Nozzle diameter = 0·167 cm: ○, $l/d = 0$; – – – –, Weber's equation; ——, modified equation. Nozzle diameter = 0·160 cm: ▽, $l/d = 49$; — — — Weber's equation.

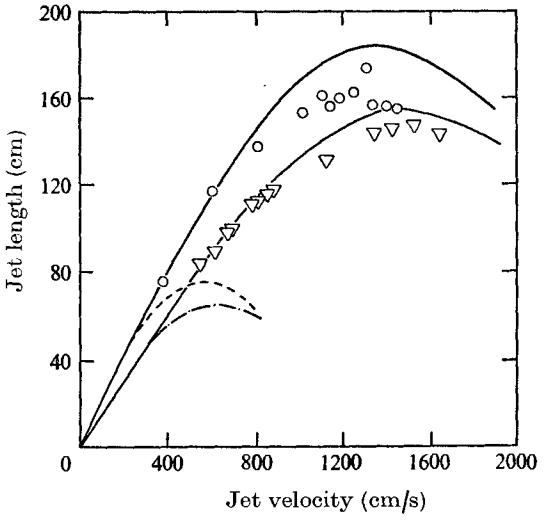

FIGURE 8. Breakup length of mineral-oil jets as a function of jet velocity and nozzle length-to-diameter ratio. Nozzle diameter = 0·167 cm: ○, $l/d = 0$; – – – –, Weber's equation; ——, modified equation. Nozzle diameter = 0·160 cm: ▽, $l/d = 49$; —·—, Weber's equation; ——, modified equation.

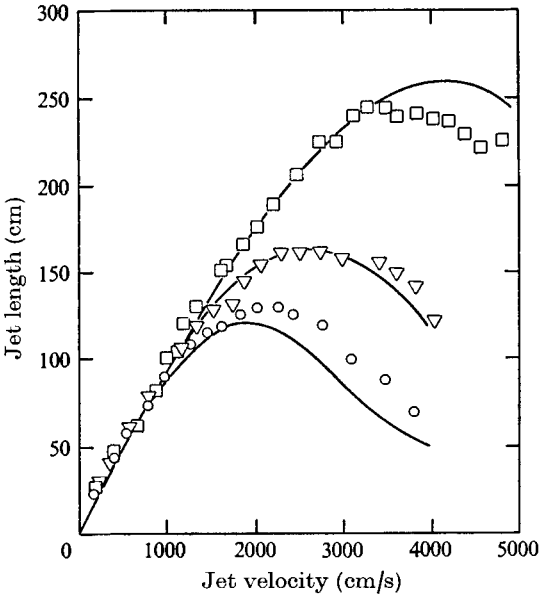

FIGURE 9. Comparison of modified equation with data of Fenn & Middleman (1969) for their solution 1, nozzle 1; Ohnesorge number $Z = 0{\cdot}372$. Ambient pressure: □, 0·2 atm; ▽, 0·5 atm; ○, 0·98 atm.

alcohol is also coincident with the occurrence of continuous surface ruffling at a Reynolds number (based on the tube diameter) between 2200 and 3000. In the case of mineral oil, however, the jet length attains a maximum at a Reynolds number of 690 in the absence of surface ruffling. The difference in the curves obtained for mineral-oil jets from the short and extended nozzles can be attributed to the contraction of the jet from the extended nozzle.

Verification of the modified theory

The modified theory is compared with experimental data in figures 4–12. These data are taken from the present experiments and from applicable results reported in the literature. Very few of the data previously reported in the literature are applicable owing to the velocity-profile relaxation effects discussed above. The exceptions are the data reported by Fenn & Middleman (1969) for liquids with viscosities of 49, 34 and 20 cP ($Z = 0{\cdot}372$, 0·262 and 0·155) and at ambient pressures of 1, 0·5 and 0·2 atm. Their results for ambient pressures of 0·067 and 0·0067 atm and their lower viscosity data are not applicable. This is indicated by the behaviour as the ambient pressure is reduced; there is little or no change in the breakup curve. Thus aerodynamic effects can no longer be the controlling factor. In view of the previous discussion this behaviour is expected for their low viscosity fluids ($Z = 0{\cdot}039$ and 0·011). While velocity-profile relaxation effects would not be expected for the high viscosity fluids at normal pressures, as the ambient density is greatly reduced, the aerodynamic forces are diminished and any contributions owing to relaxation effects are unchanged. The relaxation effects, which are negligible at normal pressures, may thus become dominant as

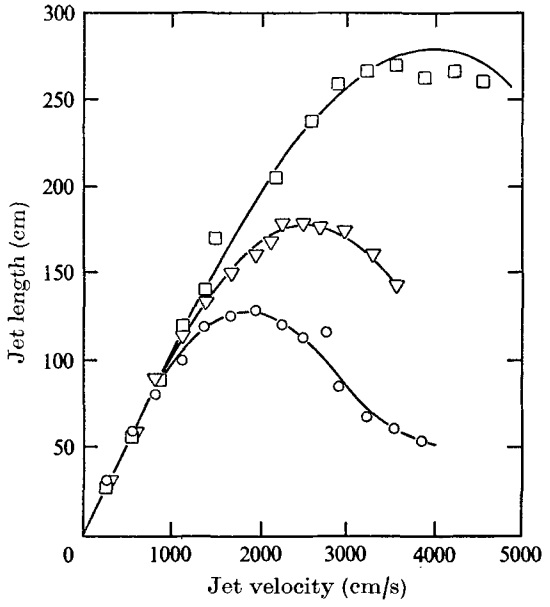

FIGURE 10. Comparison of modified equation with data of Fenn & Middleman (1969) for their solution 2, nozzle 2; Ohnesorge number $Z = 0{\cdot}262$. Ambient pressure: □, 0·2 atm; ▽, 0·5 atm; ○, 0·98 atm.

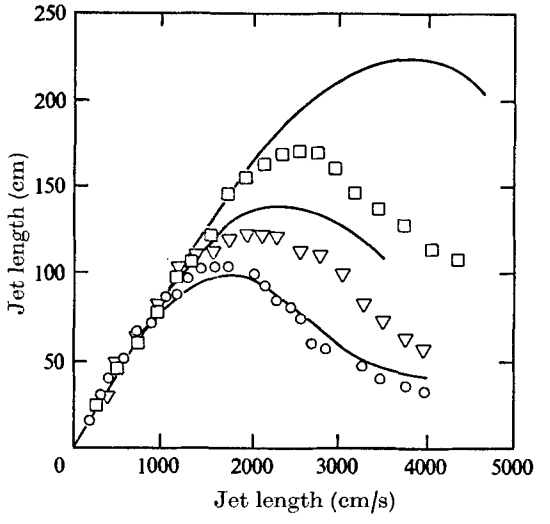

FIGURE 11. Comparison of modified equation with data of Fenn & Middleman (1969) for their solution 3, nozzle 2; Ohnesorge number $Z = 0{\cdot}155$. Ambient pressure: □, 0·2 atm; ▽, 0·5 atm; ○, 0·98 atm.

the aerodynamic forces are reduced. As can be seen in figures 9–11, this behaviour persists and is most pronounced for the lowest viscosity fluid. While the velocity-profile relaxation effects are not dominant, it is evident that they become increasingly important as the viscosity of the fluid and the ambient density are reduced.

The experimental values, in the absence of nozzle effects, of both the jet length and the jet velocity V^* at maximum length over a wide range of fluid properties, ambient densities and nozzle dimensions are correlated remarkably well by the modified theory. This is rather surprising in that Benjamin's analysis indicates that the attenuation of the aerodynamic term F_5 is not constant but rather is dependent on the Reynolds number of the ambient fluid. By considering the interdependence of the terms in the modified equation (25) and the form of Benjamin's results, we can see how this functional dependence could be reduced.

Benjamin's result implies that the attenuation constant C in the modified equation (25) should behave as

$$C = \{1 - f(\xi, \widehat{Re})\}, \tag{26}$$

where $f(\xi, \widehat{Re})$ increases as the wavenumber ξ increases and decreases as the Reynolds number $\widehat{Re}$, based on the ambient fluid properties, increases. In the limit as $\widehat{Re}$ tends uniformly to infinity, $f(\xi, \widehat{Re}) \to 0$, $C \to 1$ and the modified equation (25) reduces to Weber's equation (19). Thus we should expect C to increase with $\widehat{Re}$. We find from our calculations, however, that as the aerodynamic term CF_5 increases the wavenumber increases also. This tends to offset the effect of the ambient Reynolds number if we assume that the form (26) applies.

The wavenumber of the most unstable disturbance is an important parameter in that it determines the size of the ensuing drops. Calculations carried out using the modified equation and Weber's equation reveal a distinct relation between the wavenumber ξ^* of the most unstable disturbance and the ambient Weber number. For Weber's equation this relation is

$$\ln(\xi^*/\xi_0^*) = 0{\cdot}191\,\widehat{We},$$

and for the modified equation

$$\ln(\xi^*/\xi_0^*) = 0{\cdot}035\,\widehat{We},$$

where ξ_0^* is the dimensionless wavenumber when aerodynamic effects are absent.

These equations are compared with the experimental values of the dimensionless wavenumbers in figure 12. The experimental points are mean values of 20–108 measurements and are somewhat uncertain because of the wide scatter of the measurements about the mean values. The relative scatter of the measurements at each value of the ambient Weber number was of the order of 20%. This scatter is expected because of the random nature of the initial disturbance. Nevertheless, the modified theory shows excellent agreement with the experiment; the experimental values are correlated by the modified theory with a coefficient of correlation $r = 0{\cdot}92$.

Fenn & Middleman (1969) defined the critical ambient Weber number

$$\widehat{We}_{\text{crit}} = \hat{\rho} d U^2/\sigma$$

as the value of the ambient Weber number at which the length–velocity curve departs from a linear relationship. They determined a value of 5 from their data. It is difficult to determine this number from the data with accuracy. In addition, the error is magnified owing to the quadratic dependence on the velocity.

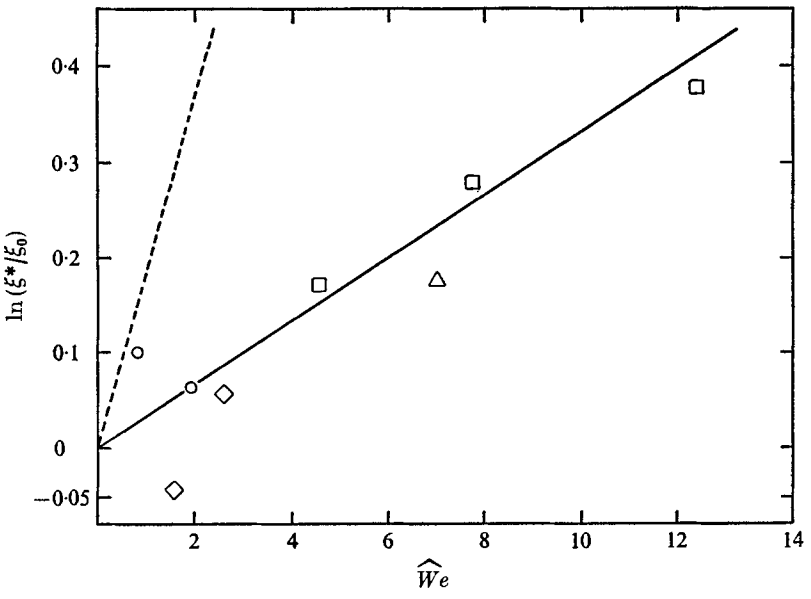

FIGURE 12. Measured and predicted variation of the dimensionless wavenumber with ambient Weber number. Nozzle diameter = 0·167 cm: △, mineral oil; □, isopropanol; ○, water. Nozzle diameter = 0·160 cm: ◇, water. – – – –, Weber's equation; ——, modified equation.

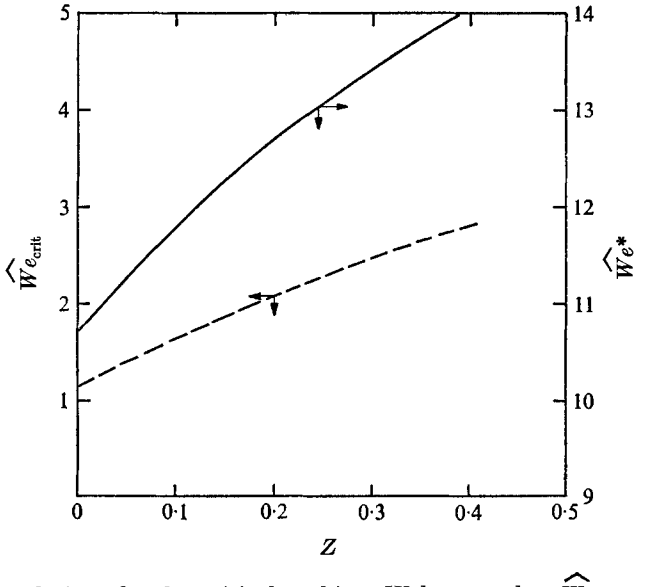

FIGURE 13. Correlations for the critical ambient Weber number $\widehat{We}_{crit}$, and the ambient Weber number $\widehat{We}^*$ at the maximum jet length as functions of the Ohnesorge number Z. These correlations were derived, by calculation, from the modified equation.

The modified equation was used to calculate the critical ambient Weber number, defined as the ambient Weber number at which the aerodynamic term is 10 % of the surface-tension term. The results of these calculations for the range $0 < Z < 0{\cdot}4$, for which the modified theory was shown to be valid, are shown in figure 13. These results suggest that a similar correlation exists for the maximum in the breakup curve, that is, that the maximum occurs when the aerodynamic term is some constant multiple of the surface-tension term. The modified theory was used to determine the values of the ambient Weber number, the aerodynamic term and the surface-tension term at the maximum in the breakup curve. Whereas these calculations show that there is no simple relationship between the aerodynamic and surface-tension terms at the maximum (perhaps owing to the subtle interaction of the terms through the wavenumber), a correlation between the ambient Weber number $\widehat{We}^*$ at the maximum jet length and the Ohnesorge number was obtained and is shown in figure 13. The experimental values of $\widehat{We}^*$ are not included as it is very difficult to determine accurately the location of the maximum in the curves because of the rather flat shape at the maximum.

6 Concluding remarks

The excellent agreement between the modified theory and the experimental results indicates that Weber's analysis of the aerodynamic effects is qualitatively correct and that, when proper consideration is given to the stresses at the jet surface, a simple modification leads to a quantitative theory. This contradicts the conclusions reached by Fenn & Middleman (1969) that: (i) Weber's analysis is not qualitatively correct, and (ii) shearing stresses at the jet surface are important.

The departure of the data of Fenn & Middleman and others from Weber's theory can be explained by the effects of velocity-profile relaxation. The criteria for determining when these effects can be ignored are yet to be established, but the present results, along with the results of Grant & Middleman, indicate that these criteria will depend on the parameter $(U^2/a^2)f(Z)$.

REFERENCES

ALTERMAN, Z. 1961 *Phys. Fluids*, **4**, 955.
BENJAMIN, T. B. 1959 *J. Fluid Mech.* **6**, 161.
BOHR, N. 1909 *Phil. Trans.* A **209**, 281.
DUDA, J. L. & VRENTAS, J. L. 1967 *Chem. Engng Sci.* **22**, 855.
FENN, R. W. & MIDDLEMAN, S. 1969 *A.I.Ch.E. J.* **15**, 379.
GAVIS, J. & MODAN, M. 1967 *Phys. Fluids*, **10**, 487.
GRANT, P. G. & MIDDLEMAN, S. 1966 *A.I.Ch.E. J.* **12**, 669.
RAYLEIGH, LORD 1878 *Proc. Lond. Math. Soc.* **10**, 4.
RUPE, J. H. 1962 *Jet Prop. Lab., Cal. Inst. Tech., Tech. Rep.* no. 32–207.
WEBER, C. 1931 *Z. angew. Math. Mech.* **11**, 136.